Proceedings of the 3rd IFAC Workshop on Automatic Control in Offshore Oil and Gas Production, Esbjerg, Denmark, May 30 - June 1, 2018

Th_C_Regular_Talk.6

On-line Fault Diagnosis of Produced Water Treatment with Multilevel Flow Modeling

Emil Krabbe Nielsen [*] Stefan Jespersen [**] Xinxin Zhang [*]
Ole Ravn [*] Morten Lind [*]

[*] *Department of Electrical Engineering, Technical University of Denmark, Elektrovej 326, Kgs. Lyngby, 2800, Denmark (e-mail: ekrani@elektro.dtu.dk).*
[**] *Department of Energy Technology, Aalborg University, Niels Bohrs Vej 8, Esbjerg, 6700, Denmark*

Abstract: Making sense of alarms can be difficult on oil and gas platforms. Multilevel Flow Modeling provides a structure for modelling plant functionality and inferring causes for alarms and predicting consequences. Currently, Multilevel Flow Modeling has limited application for on-line fault diagnosis. Based on a fault emulated on a pilot plant for offshore produced water treatment, Multilevel Flow Modeling is used for reasoning about causes for triggered alarms. The inferred causes are analysed to investigate the current maturity of Multilevel Flow Modeling for on-line diagnosis.

Keywords: Plantwide Fault Diagnosis, Multilevel Flow Modeling, Produced Water Treatment

1. INTRODUCTION

Systems for plant wide fault diagnosis of causes and effects are key to improving operator performance. For complex and safety critical systems such as offshore oil and gas production platforms, a faster and better diagnosis of faults can improve the plant safety and productivity. In this work, a Produced Water Treatment (PWT) pilot plant has been modelled with Multilevel Flow Modeling (MFM), and a fault has been emulated on the physical plant. The MFM model has been used for inferring causes to triggered alarms. The validity of the inferred causes is analysed for the emulated fault, and related to what operators experience.

Typical approaches to alarm management seek to filter, group or rank alarms (Wang et al., 2016). Instead of focusing on presenting alarms to an operator, MFM uses causal and graph based models to interprets alarms and infer root causes. An approach similar to MFM, has been used to model plant causality and isolate the root cause of plant wide oscillations. The method establishes a Signed Directed Graph from transfer entropy of process signals, and isolates the cause based on the reachability of control loops in the graph (Hu et al., 2017). Other approaches include alarm logic diagrams for identifying causes (Dubois et al., 2010; Lee et al., 2010), and Bayesian Networks for alarm prioritisation (Zhu et al., 2014). Recent focus has also been on correlation and causality methods for process signals or alarms (Yang et al., 2011, 2013).

MFM is a method for modelling goals and functions of process systems. The method has been widely applied for offline analysis of faults by Akio and Takahisa (2016); Khalil et al. (2016); Xu et al. (2015); Zhao et al. (2015); Wu et al.

(2014); Lind and Zhang (2014), as an alternative to e.g. Goal Tree Success Tree or Fault Tree Analysis (Johnson, 2013; Hurdle et al., 2007). Interest in on-line monitoring and diagnostics has increased in numerous industries over the past few years. For this reason, MFM is currently being developed to provide on-line decision support. The method has previously been applied for on-line diagnosis of power plants (Larsson et al., 2007), nuclear power plants (Larsson, 2007) and in the oil industry (Hu et al., 2015).

Currently the MFM methodology is being developed for on-line fault diagnosis for operator decision support in the oil and gas industry. Recent development includes an improved modelling methodology by Lind (2017), cause and consequence reasoning about control actions and response by Zhang and Lind (2017), causality identification from alarms by Kirchübel et al. (2017), and model performance evaluation by Nielsen et al. (2018). Initial results with on-line fault diagnosis are presented here based on the current MFM methodology.

The MFM methodology has been used to model a state of the art PWT pilot plant at Aalborg University in Esbjerg. As this plant is not used for industrial production, standard operation has been defined for the purpose of investigating the MFM methodology. For this reason, operational setpoints and alarm limits have been defined for this particular test.

2. PWT PILOT PLANT

The pilot plant at Aalborg University in Esbjerg is used for PWT. For this test the subsystems shown in the P&ID in Fig. 1 are used: support system, pipeline riser, three-phase separator and hydrocyclone. Only water and air is mixed as inflow, as no oil is used.
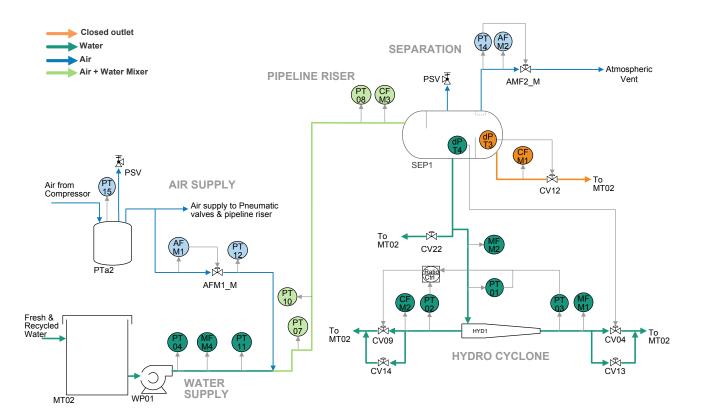
Fig. 1. P&ID of PWT Pilot Plant with the subsystems: Support, Pipeline Riser, Separator and Hydrocyclone.

The support system supplies compressed air for control valves, and air for the water mixture to emulate well gas. In addition the support system supplies water from a storage tank MT02 with a pump WP01 controlled at constant power. The water from the storage tank MT02, is recirculated back to the same storage tank MT02. The component, sensor, and valve names are shown in Fig. 1 and in Table 1. The valves CV12, CV13 and CV14 are closed during the test, whereas CV22 is closed until being used for emulating a misdirected flow.

The pipeline riser is used to deliver the mixture of water and air from the ground level in the lab to the separator. Slug control by using lift gas and a choke valve can be applied as in Pedersen et al. (2014b,a, 2017), but is not used in this test.

The three phase separator SEP1 separates the air and water delivered from the pipeline riser. A sufficiently high pressure is required to drive the water out of the separator. The separator pressure PT14 is maintained by the control valve AFM2_M at the air outlet, but also depends on the water level. The oil outlet contains no liquid and is thus closed at CV12. The control of the water level, and the hydrocyclone is in Durdevic et al. (2017) explained as two typical separate control structures for the hydrocyclone HYD1 and the three-phase separator.

The hydrocyclone is commonly used for removing smaller oil droplets from the produced water, and the separation efficiency is based on the Pressure Drop Ratio (PDR) and flow-split as described by Durdevic et al. (2017); Bram et al. (2017). The underflow control valve of the

Table 1. Pilot plant sensors and valves.

Name	System	Function
PT01	Hydrocyclone	HYD1 input pressure
PT02	Hydrocyclone	HYD1 overflow pressure
PT03	Hydrocyclone	HYD1 underflow pressure
PT04	Water support	Water support pressure
PT07	Riser	Riser bottom pressure
PT08	Riser	Riser top pressure
PT10	Riser	Riser pressure
PT11	Support	Water support pressure
PT12	Air support	Air support pressure
PT14	Separator	SEP1 pressure
PT15	Air support	Buffer tank air pressure
MFM1	Hydrocyclone	HYD1 underflow flow-rate
MFM2	Hydrocyclone	HYD1 input flow-rate
MFM4	Water support	Water support flow-rate
CFM1	Separator	SEP1 oil outlet flow-rate
CFM2	Hydrocyclone	HYD1 overflow flow-rate
CFM3	Riser	SEP1 input mixed flow-rate
AFM1	Air support	Support air flow-rate
AFM2	Separator	SEP1 air output flow-rate
dPT3	Separator	Oil level
dPT4	Separator	Water level
AFM1_M	Air Support	Control air support pressure
AFM2_M	Separator	Control PT14 SEP1 pressure
CV22	Separator	Misdirect water flow
CV04	Hydrocyclone	Control dPT4 water level
CV09	Hydrocyclone	Control PDR from PT01-03

hydrocyclone is used to control the water level of the separator, and the overflow control valve for controlling the PDR. Since oil is not used in the mixture, the quality of the PDR control is of no importance to the test.

Alarm limits have been assigned to all sensor signals. The alarm limits for the pressure sensors have been defined based on recommendations from a process expert. For those pressure sensors where the pressure influences the process performance, the limits have been defined as a deviation in percentage of 10 % for low and high, and 20 % for low low and high high. The deviation is from either the control setpoint, or the mean of 20 minutes of normal operation. All alarm limits for flow rate sensors have been defined as a deviation of a percentage from normal operation, similar to how the pressure alarms were defined. The sensor values are sampled with a frequency of 100 Hz which have been averaged to produce a signal of 1 Hz. To avoid frequent changes to alarm states, an alarm state change is acknowledged after 5 consecutive seconds. All alarm state changes which do not comply with this rule are disregarded.

3. MFM MODEL

For an overview of the MFM methodology refer to the introduction on modelling with MFM by Lind (2011), and to Zhang et al. (2013) for the rules on reasoning about causes and consequences.

The MFM model of the pilot plant shown in Fig. 2 consists of one mass flow structure, and two energy flow structures. Each flow structure contains functions, that represent the plant functionality, and the causal relations between the functions. An energy flow structure represents the conversion of electrical energy into either energy loss or rotational (kinetic energy) in the pump. The mass flow structure represents the flow of the air and water mixture, whereas the energy flow structure of the mixture, represents the energy contained in the air and water. For this reason, flow rate sensors are associated with transport functions and the water level sensor with a storage function in the mass flow structure. The pressure sensors are associated with storage functions in the energy flow structure. The functions associated with sensors are shown as blue in Fig. 2.

The model is a hypergraph of functions and objectives, connected by causal relations. Each function has a state corresponding to alarm states. Initially all states are normal during normal operation, and if an alarm is triggered as high for a pressure sensor, the corresponding storage function in MFM changes state from normal to high. This state is then propagated to adjacent functions dependent on the causal relations, to determine which functions and states could cause this change. The alarm states of all sensor signals *low low*, *low*, *normal*, *high* or *high high* are used for reasoning about potential causes.

The reasoning is triggered when an alarm state appears. MFM is then used to identify the possible root causes for all present alarm states. The purpose is thus for MFM to infer causes that are physically valid for those alarms, and in this particular case to infer that the actual root cause, the function representing CV22, has been breached.

4. EMULATED FAULT

The fault emulated on the pilot plant is a misdirected flow from CV22, between the separator and the hydrocyclone. By opening CV22 from 0 to 10 %, water is redirected from the water outlet of the separator directly to the water storage tank MT02, and thus bypasses the hydrocyclone. The first 800 seconds of the experiment is used for pressurising the three-phase separator to reach normal operation. After 900 seconds CV22 is opened by 10 %, and remains open until the system trips after 1198 seconds due to a low low water level. The following is a physical description of the consequences of the misdirected flow.

The pipe of the misdirected flow is of a larger diameter and provides a shorter return with less flow restrictions and therefore less resistance to flow. As a result of this extra pipe in parallel, more water flows out of the separator, and the separator is now in a state with a larger outflow than inflow. Due to this, the level drops steadily as shown for the signal dPT4 in Fig. 3. The control system tries to avoid this by closing CV04, but the leakage is too big; and thus CV04 closes entirely. As CV04 closes, the pressure PT03 increases. This results in the PDR controller slightly closing CV09 on average, leading to an increase of PT02 on average. However CV09, and therefore also PT02 and CFM02 oscillates due to the poorly tuned PDR controller. Closing CV04 leads to a significant decrease in flow through the hydrocyclone, as indicated in Fig. 3 for MFM01 and MFM02. The level controller keeps the control valve CV04 closed as the level stays below the setpoint of 23 cm.

As the separator pressure drops below the setpoint of 7 bars, the pressure controller closes AFM02_M. This can be seen in Fig. 3 where the flow rate of air AFM02 drops to zero.

As the water level drops, the compressed air is allowed to expand and the separator pressure PT14 drops. This drop in separator pressure means that the pump, controlled at constant power, has less resistance. As a result of the separator pressure continuously dropping, the pump can thus deliver a higher inflow rate to the separator, as can be seen for MFM04 and CFM03 on 3. At the same time, the lower separator pressure should also decrease the misdirected flow rate as there is now a lower differential pressure between the separator and the supply tank. However, the level continues to decrease, thus indicating that the misdirected flow is still larger than the inflow to the separator.

The water level continues to decrease whereas the pressure PT14 stabilizes after a while. The level in the separator is decreasing due to a larger outflow than inflow of water. The difference between the inflow and the outflow gives the rate of change of the liquid volume in the separator. As water leaves the separator the air fills out this volume by expanding. An expansion of the air leads to a decrease in pressure, and as the pressure drops; the flow rate of the separator outflow decreases whereas the inlet flow rate of air and water increases. The rate of change in volume is thus smaller, resulting in a smaller air expansion, and thus also a smaller decrease of the separator pressure PT14.
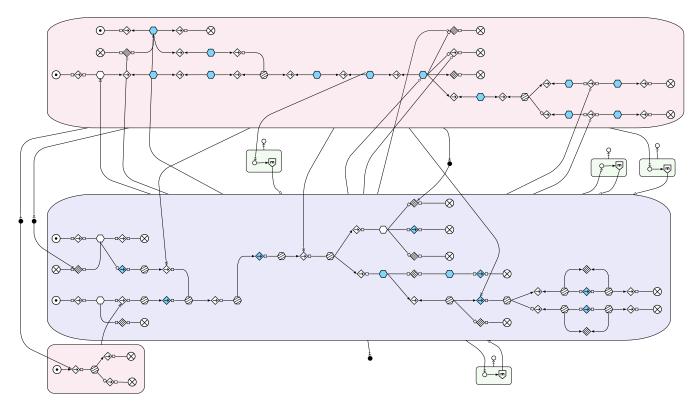
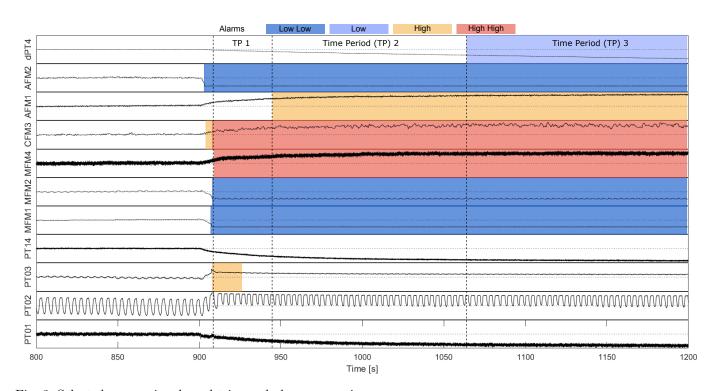Fig. 2. MFM Model of PWT Pilot Plant modelled in EGOLF.

Fig. 3. Selected sensor signals and triggered alarms over time.

At approximately 1000 s an equilibrium occurs between the expansion of the air, and the added mass of air. The pressure thus levels off even though the water level is still decreasing. As the separator pressure PT14 stops decreasing, the inlet flow rate CFM3 stabilizes.

The pressure at PT01 (the inlet of the hydroclyone) decreases in the same manner as the pressure in the separator at PT14, as it is connected to the outlet pipe of the separator. The main difference is an offset, due to the difference in hydrostatic pressure, as the flow rate is very low.

5. RESULTS

The sensor signals and the triggered alarm states are shown in Fig. 3. To simplify the presentation of the reasoning results, the test has been divided into three time periods: 908 s - 943 s, 944 s - 1062 s and 1063 s - 1998 s. In the time between 924 s and 943 s the normal alarm state of PT03 is assumed to be high to reduce the number of presented time periods.

In this section the fault will be discussed from the viewpoint of an operator, based on the triggered alarm states, and the inferred causes will be discussed in relation to the triggered alarms.

5.1 Triggered alarms

In the first period the first alarm is triggered at 902 s. The air flow rate out of the separation tank is triggered as *AFM2:Low Low*. Within the next 6 seconds, the flow rate of the mixed water and air into the separator becomes *CFM3:High*, the flow rate and pressure at the hydrocyclone underflow becomes *MFM1:Low Low* and *PT03:High*, and the input flow rate to the hydrocyclone becomes *MFM2:Low Low*. The last alarm is triggered shortly after the fault at 908 s. It is the flow rate from the pump, which increases to *MFM4:High High*. The underflow pressure alarm PT03 stops at 925 s, and the state becomes normal. However for simplicity it is considered to be high.

An operator would see more water entering the three-phase separator, but air is not leaving through the gas outlet, and the water cannot leave through the hydrocyclone underflow. The controllers indicate, that the separator air outlet valve is closed, and that the underflow valve is closed. This means that more water enters the separator, but only very little water exits through the overflow of the hydrocyclone. If more water enters the separator, but less water and air leaves it, either air or water must be leaving the separator, otherwise somewhere downstream.

In the second period, another alarm is triggered. The support system air flow rate alarm triggers as *AFM1:High* at 944 s. In addition the alarm state *PT03:High* is now normal. To the operator, the alarm PT03 can be misleading unless the operator is aware that CV04 is closed, resulting in the high pressure initially, and now that the separator pressure decreases, so does PT03. The AFM1 alarm can be difficult to draw conclusions from, but could indicate that the fault is not related to the support system, but rather something downstream, as the flow rate has increased for both the air and water in the support system, and not just the air.

In the third period, the separator water level alarm triggers as *dPT4:Low* at 1063s, 161 s after the first alarm. The current alarms stay triggered until 1198 s, after which *dPT4:Low Low* is triggered, and the system trips. This alarm should merely be a confirmation of the understanding which the operator would most likely have in the first time period. However no alarms indicate exactly from where the water leaves the separator, and it would thus be up to the operator to investigate.

5.2 Inferred causes

The reasoning results are produced by triggering the functions in the MFM model, which are associated with triggered alarm states. Based on a generic set of rules and a rule based reasoning software (Zhang et al., 2013), the states are propagated through the model to adjacent functions. The inferred causes from time period three are shown in Fig. 4. Each cause is linked to the alarms which are used as evidence to infer the specific cause. Every inferred cause may have multiple alarms as evidence. The sensors are associated with the blue functions in Fig. 2, and by triggering these functions as the alarm states, these states are then propagated to the adjacent functions. These functions are considered as the causes shown in Fig. 4. The evidence from AFM1 is not propagated to any adjacent functions, and is thus not included in the figure. It can be seen in Fig. 4 that some alarms produce more causes than other alarms, and that some causes have more alarms as evidence than other causes.
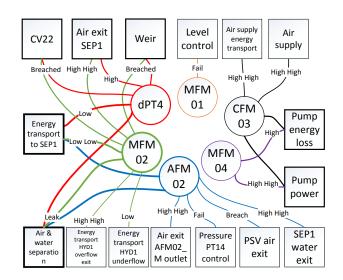

Fig. 4. Plot of causes inferred by MFM based on triggered alarm states for time period three.

The reasoning results for each time period are shown in Table 2. It can be seen in Table 2 that the actual root cause CV22 is inferred by MFM as a cause in every time period. This leaves the operator with 298 seconds to figure out, exactly which of the causes is the correct. The operator is thus introduced to the root cause at the beginning of the fault, but has to filter away all other causes, as opposed to only seeing alarms, where the operator may potentially never infer the correct cause from the alarms in this test. The number of causes inferred by MFM in each time period

ranges from 14 to 16. These causes need to be analysed by an operator by taking the current state of the plant into consideration. Instead of inferring a cause based on the alarms, the operator now has to analyse how the causes inferred by MFM correspond to the symptoms; the current alarms.

To analyse the many inferred causes, each cause has been compared to every triggered alarm state by a process expert. The comparison is shown in Table 2. An operator would be required to do something similar to identify the root cause, if presented with nothing else but a list of the 18 different causes. The expert reasons about what the plant state would be given a specific cause. If the expert agrees with an alarm state triggered in this test, a '+' has been assigned. If the alarm would not be triggered, nothing has been assigned, and if the alarm state would be opposite of the actual state a '-' has been assigned. The accuracy has been calculated for each cause, based on how many of the triggered alarms each cause agree with (Baldi et al., 2000). Only the two classes correct '+' and incorrect are used, where incorrect corresponds to both normal and '-'.

Based on this approach causes can be ranked. This however requires that corresponding alarm states are defined for as many causes as possible. Thus either process experts as in this case, or preferably data from faults are analysed to define this relationship between causes and alarm states as in Yang et al. (2011); Hu et al. (2017). This can then be used to rank causes in on-line diagnosis, or instead to improve the models in advance.

If only considering the six causes inferred by the reasoning of MFM, which has an accuracy of 0.75 and higher, only one cause is not proposed through all three time periods, and is not proposed in period one. One thing all of these six causes have in common, is that they are related to the separator. They indicate that too much water or air exits the separator, that the valve CV22 at the separator outlet has been breached or that the pressure or level controller is failing. The valve CV04 of the level control and the valve AFM2_M of the pressure control are both closed as intended. In addition the alarm state of AFM2 and MFM1 indicate either no or a very low flow rate. Thus, when valve positions are taken into account causes No. 2 and 5 seem unlikely and could be disregarded. Cause No. 3 explains that water exits the separator, but not where, whereas cause No. 1 explains exactly where. The fourth cause is air exiting the pressure safety valve. As the pressure PT14 is not near the pressure limit of the separator, air leaving through the PSV would be unintended. However if pressure would decrease because of too much air leaving the separator, the water level would be increasing, instead of decreasing.

Two of the causes have an accuracy of 0. As the overflow of the hydrocyclone has only little influence on the system, it merely affects the oil and water separation efficiency. Similarly the air and water separation influences the quality of the separation process. This corresponds to either air being part of the water fraction or water being part of the air fraction. Thus no alarms are expected to be triggered based on this, and they are only related to the process quality. The MFM model should thus be changed to better represent the hydrocyclone.

5.3 Discussion

The number of alarms and causes over time can be seen in Fig. 5. For each alarm, there are approximately two inferred causes. This becomes problematic, as the purpose is to reduce the amount of information presented to an operator, instead of increasing it. To mitigate this issue, the model size and complexity can be reduced, but the amount of different possible causes which can then be inferred, also reduces. For this reason, an index indicating the complexity, size and detail of the model, should be used in combination with a measurement of the diagnostic performance. In this way the model size is not simply reduced, just to limit the number of inferred causes presented to an operator, as the model size also introduces more different causes. Alternatively, the MFM reasoning method could be combined with alternative methods such as Bayesian Networks similar to Khalil et al. (2016) to rank causes based on probabilities.
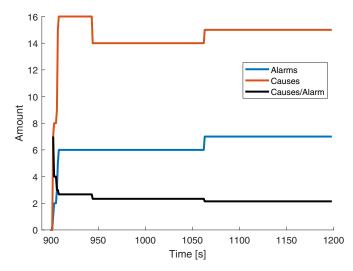
Fig. 5. Plot of triggered alarms, causes, and the ratio between causes and alarms over time.

As shown in Fig. 5, the number of causes per alarm decreases significantly in the beginning of the experiment, as more alarms trigger. This can however also be based on the reach of each alarm in the MFM model. If a function can propagate to many other functions, the causes per alarms will increase. The relationship between the number of causes and the number of alarms decreases significantly as more alarms are triggered. A low ratio is beneficial, but the total amount of causes is high, and methods for reducing the number should be developed.

There is currently no method for the MFM methodology to determine how likely one cause is over another. The MFM model proposes 16 different causes based on 6 alarms in time period 1, 14 causes based on 6 alarms in period 2 and 15 causes based on 7 alarms in period 3. This shows that MFM currently requires improvements to either the reasoning, the modelling or the alarm thresholds, in order to bring down the number of inferred causes to a reasonable level for use in decision support for operators. The authors

Table 2. Reasoning results for time periods and their validity for the triggered alarms (abbreviated names).

	Inferred cause		Period			Alarms								Accuracy
No.	Explanation	State	1	2	3	P3	M1	M2	M4	C3	A1	A2	d4	
1	CV22	Breached	x	x	x	+	+	+	+	+	+	+	+	1.00
2	Level dPT4 control	Fail	x	x	x	+	+	+	+	+	+	+	+	1.00
3	SEP1 water exit	High High	x	x	x	+	+	+	+	+	+	+	+	1.00
4	PSV air exit	Breach	x	x	x	-	+	+	+	+	+	+	-	0.75
5	Pressure PT14 control	Fail	x	x	x	-	+	+	+	+	+	+	-	0.75
6	Air exit SEP1	High			x	-	+	+	+	+	+	+	-	0.75
7	Air trans SEP1 air outlet	High High	x	x	x	-	+	+	+	+	+	-	-	0.63
8	Pump energy loss	High	x	x	x	+	+	+	-	-	+	-		0.50
9	Energy trans HYD1 underflow	Low	x	x	x	+	+	+						0.38
10	Energy trans HYD1 input	High	x			+	-	-	+	+		-		0.38
11	Pump power	High High	x	x	x	-	-	-	+	+			-	0.25
12	Air supply energy trans.	High	x	x	x					+	+			0.25
13	Water trans SEP1 outlet	Low Low	x	x		-	+	+	-	-	-	-	-	0.25
14	Overflow energy transport	Low	x			+	-	+				-		0.25
15	Energy transport to SEP1	Low	x	x	x							+		0.13
16	Weir	Breached			x	-	-	-	-	-	-	-	+	0.13
17	Energy trans HYD1 overflow	High High	x	x	x									0.00
18	Air and water separation	Leak	x	x	x									0.00

suggest the following solutions to reduce the number of causes presented:

(1) A method for validating models according to triggered alarms could improve the cause predictions for on-line fault diagnosis with MFM models. Causal relations of models are thus revised so that inferred causes correspond to the triggered alarms to a higher degree.

(2) A method for cause ranking, filtering, grouping or something similar would be beneficial to automatically falsify or reduce the number of inferred causes.

(3) Alternative methods to traditional alarms for triggering functions in models. E.g. thresholds for MFM models only.

Currently, a causal relation is established between two functions of an MFM model, if one function can influence the other. When modelling, there is no consideration of the magnitude of influence. The validation approach would require that numerous faults are emulated or simulated, so that process experts would not be involved in comparing alarm states to causes, as done in this approach to produce Table 2. Based on the emulated and simulated data, the causal relations in the MFM models should be updated, so that specific causes do not appear for specific alarms. The causal relations would then be established based on whether a change of one function can cause a deviation of another function, significantly large to trigger an alarm or compromise the safety of the plant. However, the MFM model loses its property of generalizing plant behaviour, the more strictly this approach is applied.

6. CONCLUSION

A produced water treatment pilot plant has been modeled with Multilevel Flow Modeling, for the purpose of on-line fault diagnosis for operator decision support. A fault has been emulated on the plant, by opening a closed valve such that the water flow is misdirected. The alarms triggered over time, are used as evidence for defining state changes of MFM functions.

The MFM model represents the system well for this specific fault, as the majority of the inferred causes to some degree comply with the alarms triggered by the fault. The majority of causes have discrepancies with the triggered alarms, except for the actual root cause. Multilevel Flow Modeling is capable of inferring the root cause of the emulated fault. For presentation of the results, they have been divided into three time periods. The root cause is inferred by MFM in all three time periods leaving the operator with a potential of 298 seconds to react.

The MFM model produces approximately two causes per alarm for this fault. The amount of information thus increases compared to only using alarms. For this reason model validation based on emulated or simulated faults is suggested, instead of solely relying on input from process experts. In addition cause filtering, ranking or grouping should be introduced along with an index indicating the model complexity.

REFERENCES

Akio, G. and Takahisa, I. (2016). Functional information in operator support systems. *Nuclear Safety and Simulation*, 7(1), 35–41.

Baldi, P., Brunak, S., Chauvin, Y., Andersen, C.A.F., and Nielsen, H. (2000). Assessing the Accuracy of Prediction Algorithms for Classification: An Overview. *Bioinformatics*, 16(5), 412–424. doi:10.1093/bioinformatics/16.5.412.

Bram, M.V., Hansen, L., Hansen, D.S., and Yang, Z. (2017). Grey-box modeling of an offshore deoiling hydrocyclone system. In *2017 IEEE Conference on Control Technology and Applications (CCTA)*, 94–98. doi:10.1109/CCTA.2017.8062446.

Dubois, L., Fort, J.M., Mack, P., and Ryckaert, L. (2010). Advanced logic for alarm and event processing: Methods to reduce cognitive load for control room operators. *IFAC Proceedings Volumes*, 43(13), 158 – 163. doi: doi.org/10.3182/20100831-4-FR-2021.00029.

Durdevic, P., Pedersen, S., and Yang, Z. (2017). Challenges in Modelling and Control of Offshore De-oiling

Hydrocyclone Systems. *Journal of Physics: Conference Series*, 783(1).

Hu, J., Zhang, L., Cai, Z., and Wang, Y. (2015). An intelligent fault diagnosis system for process plant using a functional HAZOP and DBN integrated methodology. *Engineering Applications of Artificial Intelligence*, 45, 119–135. doi:10.1016/j.engappai.2015.06.010.

Hu, W., Shah, S.L., and Chen, T. (2017). Framework for a smart data analytics platform towards process monitoring and alarm management. *Computers & Chemical Engineering*. doi: doi.org/10.1016/j.compchemeng.2017.10.010.

Hurdle, E.E., Bartlett, L.M., and Andrews, J.D. (2007). System fault diagnostics using fault tree analysis. *Proceedings of the Institution of Mechanical Engineers, Part O: Journal of Risk and Reliability*, 221(1), 43–55. doi: 10.1243/1748006XJRR6.

Johnson, S.B. (2013). Goal-function tree modeling for systems engineering and fault management. In *AIAA Infotech@Aerospace (I@A) Conference*, 1–13. doi: 10.2514/6.2013-4576.

Khalil, M.A., Ahmad, A., Abdullah, T.A.T., and Al-shanini, A. (2016). Failure Analysis Using Functional Model and Bayesian Network. *Chemical Product and Process Modeling*. doi:10.1515/cppm-2016-0007.

Kirchübel, D., Zhang, X., and Lind, M. (2017). Identifying Causality from Alarm Observations. In *International Symposium on Future Instrumentation and Control for Nuclear Power Plants*, 1–6.

Larsson, J.E. (2007). On-Line Root Cause Analysis For Nuclear Power Plant Control Rooms. In *Proceedings of the International Symposium on Symbiotic Nuclear Power Systems for the 21st Century*. Fukui, Japan.

Larsson, J.E., Öhman, B., and Calzada, A. (2007). Real-Time Root Cause Analysis for Power Grids. In *Secutiry and Reliability of Electric Power Systems*, 1–7.

Lee, J.W., Kim, J.T., Park, J.C., Hwang, I.K., and Lyu, S.P. (2010). Computer-based alarm processing and presentation methods in nuclear power plants. *World Academy of Science, Engineering and Technology*, 41, 594–598.

Lind, M. (2011). An introduction to multilevel flow modeling. *Nuclear safety and simulation*, 2(1), 22–32.

Lind, M. (2017). Knowledge Acquisition and Strategies for Multilevel Flow Modelling. In *International Symposium on Future Instrumentation and Control for Nuclear Power Plants*.

Lind, M. and Zhang, X. (2014). Functional Modelling for Fault Diagnosis and its Applications for NPP. *Nuclear Engineering and Technology*, 46(6), 753–772. doi: 10.5516/NET.04.2014.721.

Nielsen, E.K., Bram, M.V., Frutiger, J., Sin, G., and Lind, M. (2018). A water treatment case study for quantifying model performance with multilevel flow modeling. *Nuclear Engineering and Technology*. doi: 10.1016/j.net.2018.02.006.

Pedersen, S., Stampe, K., Pedersen, S.L., Durdevic, P., and Yang, Z. (2014a). Experimental study of stable surfaces for anti-slug control in multi-phase flow. In *2014 20th International Conference on Automation and Computing*, 43–48. doi:10.1109/IConAC.2014.6935458.

Pedersen, S., Durdevic, P., and Yang, Z. (2014b). Learning control for riser-slug elimination and production-rate

optimization for an offshore oil and gas production process. *IFAC Proceedings Volumes*, 47(3), 8522 – 8527. doi: doi.org/10.3182/20140824-6-ZA-1003.0249. 19th IFAC World Congress.

Pedersen, S., Løhndorf, P.D., and Yang, Z. (2017). Influence of riser-induced slugs on the downstream separation processes. *Journal of Petroleum Science and Engineering*, 154(Supplement C), 337 – 343. doi: doi.org/10.1016/j.petrol.2017.04.042.

Wang, J., Yang, F., Chen, T., and Shah, S.L. (2016). An overview of industrial alarm systems: Main causes for alarm overloading, research status, and open problems. *IEEE Transactions on Automation Science and Engineering*, 13(2), 1045–1061. doi: 10.1109/TASE.2015.2464234.

Wu, J., Zhang, L., Hu, J., Lind, M., Zhang, X., Jørgensen, S.B., Sin, G., and Jensen, N. (2014). An Integrated Qualitative and Quantitative Modeling Framework for Computer-Assisted HAZOP Studies. *American Institute of Chemical Engineering*, 60(12), 4150–4173. doi: 10.1002/aic.14593.

Xu, Y., Wang, D., Wang, J., Wang, J., Hu, L., and Yang, Z. (2015). Fault Diagnosis of HCCB TES for ITER Based on Functional Modeling. *Journal of Fusion Energy*, 34(6), 1489–1496. doi:10.1007/s10894-015-9973-9.

Yang, F., Shah, S.L., Xiao, D., and Chen, T. (2011). Improved correlation analysis and visualization of industrial alarm data. *IFAC Proceedings Volumes*, 44(1), 12898 – 12903. doi:doi.org/10.3182/20110828-6-IT-1002.03193. 18th IFAC World Congress.

Yang, Z., Wang, J., and Chen, T. (2013). Detection of correlated alarms based on similarity coefficients of binary data. *IEEE Transactions on Automation Science and Engineering*, 10(4), 1014–1025. doi: 10.1109/TASE.2013.2248000.

Zhang, X. and Lind, M. (2017). Reasoning about Cause-effect through Control Functions in Multilevel Flow Modelling. In *International Symposium on Future Instrumentation and Control for Nuclear Power Plants*, 1–8.

Zhang, X., Lind, M., and Ravn, O. (2013). Consequence reasoning in multilevel flow modelling. In *IFAC Symposium on Analysis, Design and Evaluation of Human-Machine Systems*, 187–194. IFAC, Las Vegas, USA. doi: 10.3182/20130811-5-US-2037.00028.

Zhao, Y., Jiao, J., and Zhao, T. (2015). A functional hazard analysis based on Multilevel Flow Modeling. *Engineering Management and Industrial Engineering*, (November), 75–80. doi:10.1201/b18407-17.

Zhu, J., Zhao, J., and Yang, F. (2014). Dynamic risk analysis with alarm data to improve process safety using bayesian network. In *Proceeding of the 11th World Congress on Intelligent Control and Automation*, 461–466. doi:10.1109/WCICA.2014.7052757.